

# Gigahertz Analog Repeater for Fiber Optic Delay Lines

CHING-TEN CHANG

**Abstract**—A gigahertz analog fiber optic repeater is used to extend the achievable delay time for radar delay line applications. The repeater consists of a silicon avalanche photodiode (APD), a wide-band amplifier, and a GaAlAs laser diode transmitter. This repeater has an optical gain of 14.5 dB, a 42 dB electrical dynamic range, and a noise figure of approximately 6.5 dB. The frequency response is flat within  $\pm 2$  dB over the frequency range from 10 MHz to 1.3 GHz. The nanosecond pulse fidelity is such that the subtraction between input and output pulses is 20 dB below the pulse amplitude.

## I. INTRODUCTION

To avoid the multipath propagation effects due to reflection from the sea surface, shipboard radar must be operated at a high frequency (such as *K*-band) for the detection of low-flying targets. However, a conventional coherent moving-target indicator (MTI) is difficult to operate at such a high frequency [1]. An alternate approach is a noncoherent MTI based on subtraction of radar returns from two successive pulses [2], using a fiber optic delay line as a delay medium. This pulse-to-pulse subtraction will retain the moving target signal returns and reject the stationary clutter returns. A radar pulse of 1 ns width (after pulse compression) and 1 ms separation (pulse repetition interval) can detect low flyers with radial speed greater than about 500 ft/s.

The required fiber optic delay line length is 200 km for 1 ms delay. Only fiber optic delay lines appear to have the real-time capacity for preserving the 1 ns pulse after 1 ms delay. Because of finite fiber attenuation ( $\sim 2.5$  dB/km at  $0.85 \mu\text{m}$ ), it is impossible to transmit a 1 ns pulse over such a long fiber. Thus, a gigahertz analog fiber optic repeater is needed to strengthen the optical pulse amplitude during its transmission. This repeater consists of an avalanche photodiode (APD) receiver, a wide-band amplifier, and a laser diode transmitter.

A weak input optical pulse is detected by the APD receiver and amplified. The amplified pulse is used to drive the transmitter to generate a strong output optical pulse. Repeater performance characteristics pertaining to the radar MTI application are investigated. These include pulse fidelity, linearity, dynamic range, noise figure, and frequency response. Good agreement between experimental measurements and analytical predictions is obtained on the repeater dynamic range and repeater noise figure.

Manuscript received October 5, 1981; revised December 1, 1981. This work was supported by NAVSEA Radar Block Program and the Naval Research Laboratory.

The author is with the Department of Electrical Engineering, San Diego State University, San Diego, CA 92182, and the Naval Ocean Systems Center, San Diego, CA 92152.

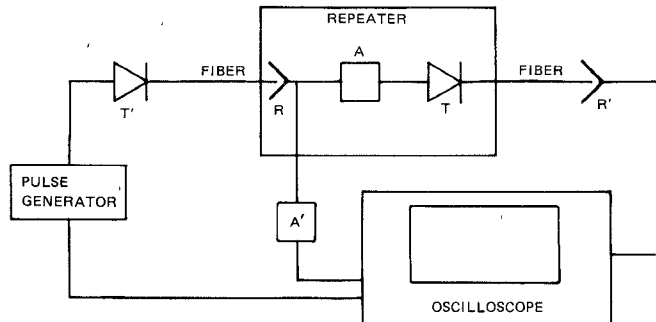


Fig. 1. Block diagram of the experimental setup for a gigahertz analog fiber repeater. This repeater consists of an APD receiver  $R$ , a cascaded amplifier  $A$ , and a laser diode transmitter  $T$ .

## II. EXPERIMENTAL CHARACTERIZATION OF THE REPEATER

Fig. 1 shows the repeater consisting of an avalanche photodiode receiver  $R$ , a cascaded amplifier  $A$ , and a laser diode transmitter  $T$ . The APD receiver  $R$  has a quantum efficiency of approximately 60 percent and a bandwidth of several gigahertz. The avalanche gain  $M$ , defined as the ratio of avalanche photocurrent to primary photocurrent, is measured to be  $M = 39$ . The amplifier used in the repeater is composed of Walkins-Johnson models 6023-327 and 6023-432 in series, with the 6023-432 as the output stage. This cascaded amplifier provides 50 dB gain. The laser diode transmitter  $T$  is the General Optronics model GOLT-3 with a single-mode optical fiber pigtail. The slope of the static light versus current ( $L$ - $I$ ) curve is 5 mW/mA with a dc biasing current of 70 mA, and the lasing threshold is approximately 64 mA. This biasing above the lasing threshold is necessary in order to obtain a subnanosecond laser response.

In order to evaluate the repeater performance, additional laser transmitter  $T'$  and the APD receiver  $R'$  are utilized for generation of the repeater input optical pulses and for detection of the repeater output optical pulses, respectively (see Fig. 1). Both biasing current and pulsing current of the transmitter  $T'$  are fixed during the experimental characterization of the repeater. The ratio between pulsed optical power  $P_i$  and biasing (dc) optical power  $P_{bi}$  is measured to be  $P_i/P_{bi} = 1.35$ . The avalanche gain of the APD receiver  $R'$  is measured to be  $M' = 45.1$ .

Typical pulse responses of the repeater are shown in Fig. 2. Here the top trace is the detected input optical pulse amplified by the amplifier  $A'$  with 30 dB gain and the bottom trace is the detected output optical pulse. The central trace shows the

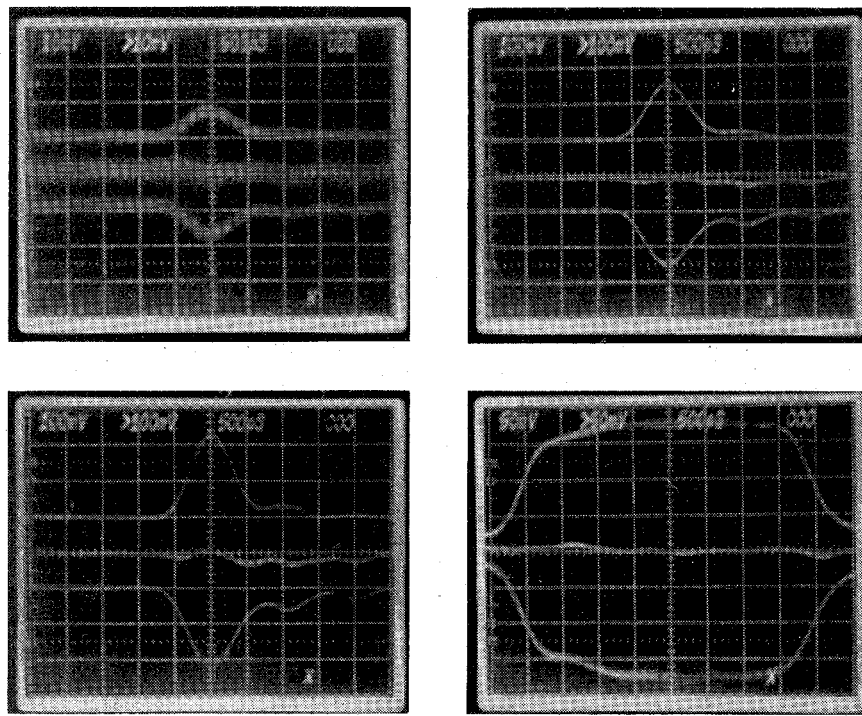


Fig. 2. Various pulse responses of the repeater. Top trace is the detected (by  $R$ ) input optical pulse after 30 dB amplification, while the bottom trace is the detected (by  $R'$ ) output optical pulse. The central trace is the difference between input and output pulses. The electrical gain of the repeater is 30 dB, while the optical gain is about 15 dB.

difference indicating the fidelity of the repeater is such that the pulse amplitude difference is typically 20 dB below the input or output pulses. The repeater (electrical) gain is approximately 30 dB.

The repeater linearity is shown in Fig. 3. Various input and output levels are obtained by changing the repeater input optical coupling between  $T'$  and  $R$ . This simulates input optical pulses under various optical fiber attenuations before their arrivals at the repeater. The repeater is linear from 1.8 to 215 mV. Here, 1.8 mV is the minimum detectable output pulse with  $(S/N)_o = 1$ , and 215 mV is the maximum output pulse with 3 dB compression in the repeater gain.

Noises of optical pulses are assumed to be Gaussian distributed. The root-mean-square noise voltage  $\sigma$  is measured by the tangential method [3] using a Tektronix 7104 oscilloscope with gigahertz real-time capacity. The signal-to-noise ratio in decibels is

$$\left( \frac{S}{N} \right) = 20 \log_{10} \frac{V_p}{\sigma}$$

where  $V_p$  is the detected optical pulse amplitude. This tangential method relies on the fact that two identical Gaussian distributed curves form just a single curve with uniform trace intensity, when the curves are separated by exactly two rms noise voltage ( $2\sigma$ ). The point at which this occurs is independent of the height of the curves, the length of observation, or the scope intensity [3].

The measured repeater input signal-to-noise ratio  $(S/N)_i$  as a function of the input pulse amplitude is shown in Fig. 4, while the corresponding repeater output signal-to-noise ratio  $(S/N)_o$  is shown in Fig. 5. The noise figure for the repeater, indicating the ratio of  $(S/N)_i$  to  $(S/N)_o$ , is shown in Fig. 6. The input

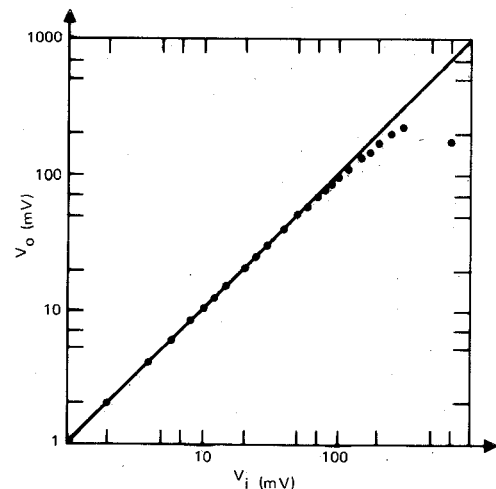


Fig. 3. Repeater output amplitude ( $V_o$ ) versus repeater input amplitude ( $V_i$ ). This figure shows the repeater linearity.

noises in Figs. 4 and 6 include both the input repeater noise and the noise generated by the amplifier  $A'$ . The amplifier  $A'$  is needed because the input pulse without amplification is weak and is not suitable for the measurement of input signal-to-noise ratio over the oscilloscope. Assuming the amplifier  $A'$  has a noise figure of 4 dB, then the measured repeater  $(S/N)_i$  and noise figure should be 4 dB up in Figs. 4 and 6.

The frequency response of the repeater consisting of the amplifier  $A$ , transmitter  $T$ , and receiver  $R'$  is shown in Fig. 7. This frequency response is linear within  $\pm 2$  dB from 10 MHz to 1.3 GHz. The laser biasing is set to be 80 mA so that the laser is never operating below its lasing threshold during the process of swept frequency measurement using a spectrum analyzer.

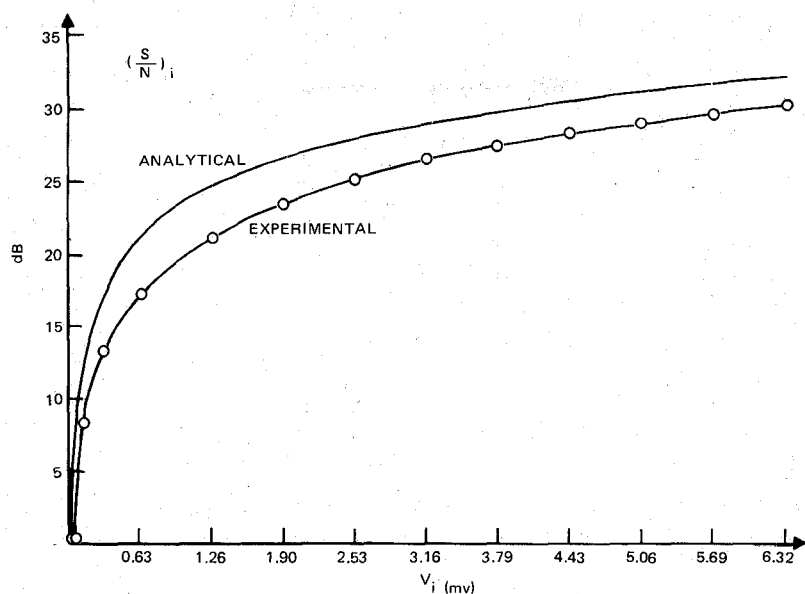


Fig. 4. Input signal (or pulse amplitude) to noise ratio  $(S/N)_i$  as a function of input pulse amplitude  $V_i$ . The measured  $(S/N)_i$  includes the noise contribution from the amplifier  $A'$  (see Fig. 1). The real repeater  $(S/N)_i$  without noise contribution from the amplifier  $A'$  is approximately 4 dB higher than that shown in this figure.

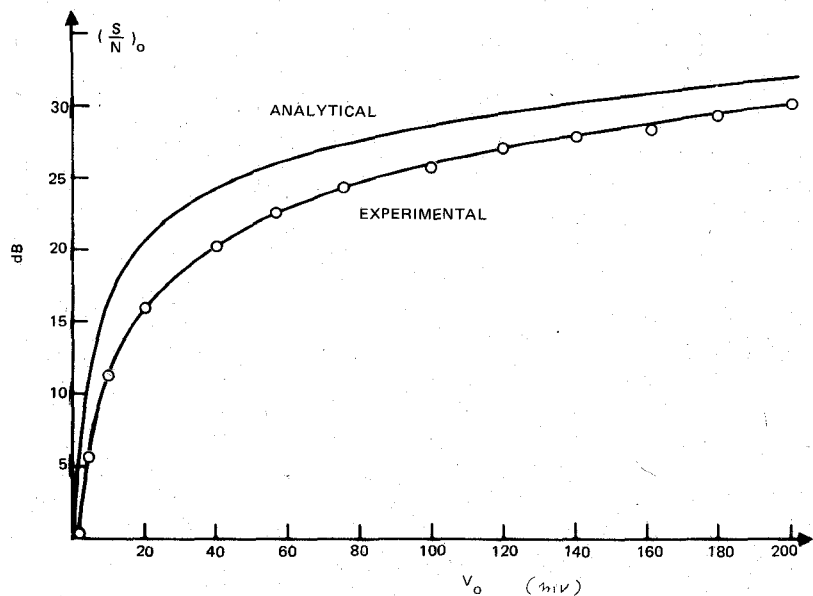


Fig. 5. Output signal (or pulse amplitude) to noise ratio  $(S/N)_o$  as a function of output pulse amplitude  $V_o$ .

### III. ANALYSIS OF THE REPEATER PERFORMANCE

Input optical pulses are composed of pulsed optical power  $P_i$  and dc biasing optical power  $P_{bi} = P_i/1.35$  in our experiments. The signal-to-noise ratio  $(S/N)_i$  for the detected optical pulse using the avalanche photodiode  $R$  is [4]

$$\left(\frac{S}{N}\right)_i = \frac{(MrP_i)^2}{2eF(M)M^2r(P_i + P_{bi})B + 4kTB/R_i} \quad (1)$$

Here  $B = 10^9$  Hz is the overall bandwidth for detection and display of optical pulses,  $R_i = 50 \Omega$  represents the input impedance of the amplifier  $A$  or  $A'$ ,  $e$  is the electronic charge,  $r = 0.41$  A/W, and  $M = 39$  are the primary photoelectron responsivity and avalanche gain of the APD receiver  $R$ , respectively, and  $F(M)$  is the APD excess noise factor. Assuming the impact ionization ratio [4] of holes to electrons is  $k = 0.035$

in silicon APD's, this noise factor can be written as

$$F(M) = kM + \left(2 - \frac{1}{M}\right)(1 - k). \quad (2)$$

The repeater input signal displayed over the oscilloscope with  $50 \Omega$  input impedance becomes input signal voltage

$$V_i = 50 MrP_i. \quad (3)$$

Fig. 4 shows  $(S/N)_i$  versus  $V_i$  for input optical pulses obtained from (1)-(3). This analytical curve is in reasonable agreement with the measured curve.

The repeater has an experimental gain of 30 dB (voltage gain of 31.6). Thus the output signal voltage  $V_o$  is

$$V_o = 1580 MrP_i. \quad (4)$$

This output optical pulse is detected by the APD receiver  $R'$

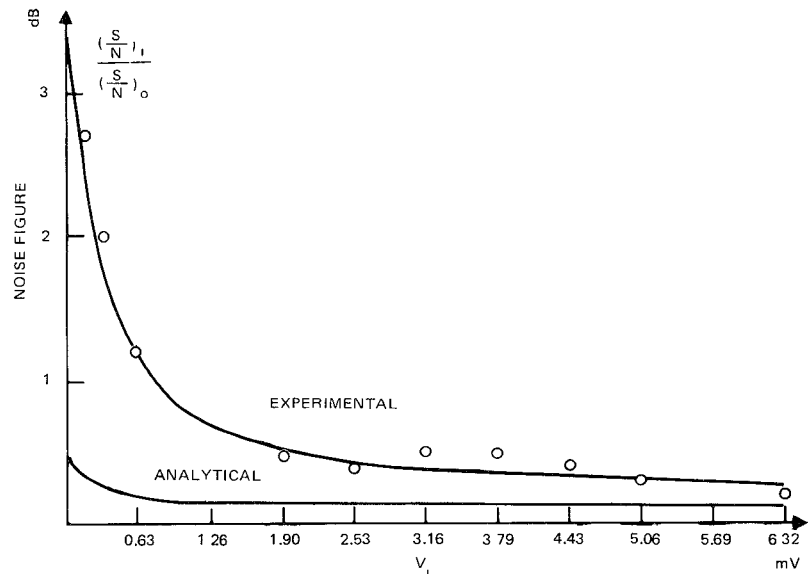


Fig. 6. Repeater noise figure (NF) as a function of input pulse amplitude  $V_i$ . The measured noise figure shown includes the noise contribution from the amplifier  $A'$ . The real repeater NF is approximately 4 dB higher than this measured NF shown in the figure.

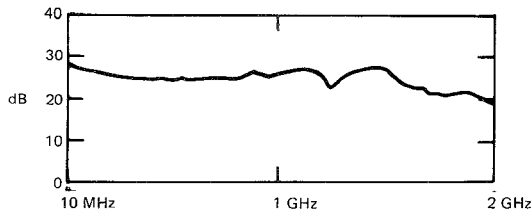


Fig. 7. Frequency response of the repeater from 10 MHz to 2 GHz. One vertical division corresponds to 10 dB.

with an avalanche gain  $M' = 45.1$  and an assumed responsivity  $r' = 0.41$  A/W. Dividing (4) by  $50 M' r'$ , we obtained the pulsed optical output power  $P_o$  from the transmitter  $T$  as

$$P_o = 27.3 P_i. \quad (5)$$

This means that the optical power gain of the repeater is 27.3, which is different from the voltage gain of 31.6 due to different avalanche gains between the receivers  $R$  and  $R'$ . The signal-to-noise ratio  $(S/N)_o$  for the detected output optical pulse is

$$\left(\frac{S}{N}\right)_o = \frac{(M' r' P_o)^2}{2eF(M')M'^2 r'(P_o + P_{bo}) B + [2eF(M)M^2(P_i + P_{bi})rB + 4kTB/R_i] 1000} \quad (6)$$

where  $P_{bo} = 38 \mu\text{W}$  is the dc biasing power of the transmitter  $T$  measured at the pigtail fiber end. The first term in the denominator is the noise of the APD receiver  $R'$  with  $F(M') = 3.49$ , while the second term is the input noises from both the receiver  $R$  and the  $50 \Omega$  input resistance of the amplifier  $A$  and then amplified by 30 dB repeater gain. The repeater output  $(S/N)_o$  as a function of the repeater output voltage  $V_o$ , calculated from (4)–(6), is shown in Fig. 5. The difference in decibels between Figs. 4 and 5 is shown in Fig. 6. This is the analytical noise figure of the repeater.

#### IV. DISCUSSION

Maximum and minimum detected output optical pulses are measured to be 215 and 1.8 mV, respectively. Thus the repeater dynamic range defined as the ratio of maximum to minimum detectable optical pulses is 42 dB. The minimum detectable optical pulse can be predicted by letting  $(S/N)_o = 1$  in (6) and then solving it together with (5). The analytical result is  $P_o = 1 \mu\text{W}$  or  $V_o = 0.95 \text{ mV}$  which is about half of the observed value of 1.8 mV. Two dominant noise currents at the repeater output are 1) the thermal noise of the  $50 \Omega$  amplifier input resistance under 30 dB repeater gain;  $\langle i_t^2 \rangle = 3.25 \times 10^{-10} \text{ A}^2$  and 2) the shot noise produced by the biasing optical power  $P_{bo} = 38 \mu\text{W}$ ;  $\langle i_q^2 \rangle = 3.5 \times 10^{-11} \text{ A}^2$ . The maximum optical pulse is limited by the laser power saturation as well as by the coupling efficiency between the laser diode and its single-mode optical fiber pigtail.

When the output laser diode transmitter  $T$  is biasing above threshold, the slope of the static  $L$ - $I$  curve is 5 mW/mA. If the input optical power  $P_i$  is detected by the APD receiver  $R$  with  $M = 39$  and  $r = 0.41$  A/W and subsequently amplified by the

amplifier  $A$  with 50 dB gain (or 316 current gain), then the output optical power  $P_o$  based on the static  $L$ - $I$  curve becomes  $P_o = 25.3 P_i$ . This repeater gain is less than the measured gain of 27.3, probably due to the difference between static and dynamic  $L$ - $I$  curves. Typical optical pulses in the experiment are of nanosecond duration and 3  $\mu\text{s}$  separation. This then makes the slope of dynamic  $L$ - $I$  curve larger than the corresponding static slope of 5 mW/mA, since the thermal effect is negligibly small in this low duty nanosecond pulse operation.

The problems encountered in the evaluation of this gigahertz

analog fiber optic repeater are laser relaxation oscillation and laser self-pulsation [5]. Both relaxation oscillation and self-pulsation cause an appreciable difference between input and output repeater pulses. This then makes the task of the analog repeater difficult. Another problem encountered is laser degradation during the process of experimental repeater characterization. That is to say the nonself-pulsating laser develops the problem of self-pulsation after lasing for some time. The problem of self-pulsation is finally overcome by choosing a laser with low  $Q$  cavity [6]. However, this low  $Q$  laser has less power output and causes the dynamic range to be a little lower than expected.

The present repeater has an optical gain of 14.4 dB (or 27.3), an electrical dynamic range of 42 dB, and a noise figure of approximately 6.5 dB. This would allow the analog recirculation of 1 ns pulse through a 5 km fiber with 2.8 dB/km attenuation possible by considering the optical power budget only. The signal-to-noise ratio at the maximum signal amplitude is 30 dB (see Fig. 5). That is less than 42 dB because of optical signal generated noise [see (6)]. As a result of the analog noise accumulation in the process of recirculation, the maximum number of analog recirculation will be  $\sim 2$ . After two recirculations the signal-to-noise ratio will be 17 dB ( $\approx 30 - 2 \times 6.5$ ). This implies that much more than two times recirculation is difficult. In order to achieve 1 ms delay of a 1 ns pulse, it is necessary to recirculate 39 times through the 5 km fiber optic delay line at 0.85  $\mu\text{m}$ . An alternate way to achieve this long delay (1 ms) is to digitize the radar returns. Digital (binary) transmission can avoid the problem of analog noise accumulation in the repeater [7]. The regenerated digital signal can be free from error, provided that the signal-to-noise ratio is  $\geq 20$  dB before the process of digital regeneration.

It is well known that single-mode fiber attenuation and dispersion are both minimized at the long wavelength region. The best fiber attenuations [8] reported to date are 0.5 dB/km at 1.3  $\mu\text{m}$  and 0.2 dB/km at 1.55  $\mu\text{m}$ . The single-mode fiber dispersion can also be minimized at these two wavelengths by properly choosing the fiber parameters to obtain a cancellation [8], [9] between material and waveguide dispersions. Dispersionless transmission of 2 Gbit/s signals over a 44.3 km single-mode fiber at 1.3  $\mu\text{m}$  has been demonstrated recently with  $10^{-9}$  error rate [10]. Thus the long wavelength single-mode fiber will be the ideal candidate for analog wideband radar delay line applications.

## ACKNOWLEDGMENT

The author would like to thank R. Patterson, S. Pappert, and M. Feinstein for their technical aid, G. M. Dillard, H. F. Taylor, F. J. Harris, C. J. Hwang, and G. Massey for their technical discussions, and H. E. Rast, M. S. Lin, and J. H. Harris for their encouragement.

## REFERENCES

- [1] C. T. Chang, D. E. Altman, D. R. Wehner, and D. J. Albares, "Noncoherent radar moving target indicator using fiber optic delay lines," *IEEE Trans. Circuits Syst.*, vol. CAS-26, pp. 1132-1135, 1979.
- [2] B. H. Cantrell, "A short-pulse area MTI," Naval Research Laboratory, Washington, DC, Rep. 8162, Sept. 1977.
- [3] G. Franklin and T. Hatley, "Don't eyeball noise," *Electron. Des.*, vol. 24, pp. 184-187, 1973.
- [4] R. G. Smith and S. D. Personick, in *Semiconductor Devices for Optical Communication*, H. Kressel, Ed. New York: Springer-Verlag, 1979, ch. 4.
- [5] I. P. Kaminow and T. Li, in *Optical Fiber Telecommunications*, S. E. Miller and A. G. Chynoweth Eds. New York: Academic, 1979, ch. 17.
- [6] C. J. Hwang, private communication.
- [7] A. Yariv, *Introduction to Optical Electronics*. New York: Holt, Rinehart and Winston, 1976, ch. 11.
- [8] T. Kimura, "Single-mode digital transmission technology," *Proc. IEEE*, vol. 68, pp. 1263-1268, 1980.
- [9] C. T. Chang, "Minimum dispersion in a single-mode step-index optical fiber," *Appl. Opt.*, vol. 18, pp. 2516-2521, 1979.
- [10] J. I. Yamada, S. Machida, and T. Kimura, "2 Gbit/s optical transmission experiments at 1.3  $\mu\text{m}$  with 44 km single-mode fiber," *Electron. Lett.*, vol. 17, pp. 479-480, 1981.



Ching-Ten Chang received the B.S. degree in physics from the National Taiwan Normal University in 1966, the M.S. degree in physics from North Dakota State University, Fargo, in 1969, and the Ph.D. degree in electrical engineering from the University of Washington, Seattle, in 1975.

As a Research Associate with the University of Washington from 1975 to 1977, he conducted research in fiber optics, optical holography, and photoacoustic spectroscopy. He joined the Naval Ocean Systems Center as an Electronic Engineer in 1977. Since then his research interests have been in optical fiber communications, fiber optic delay lines, and heterostructure lasers. He is currently an Associate Professor at the Department of Electrical Engineering, San Diego State University, San Diego, CA.